

ACCURACY ANALYSIS OF PHOTGRAMMETRICALLY DERIVED POINT
CLOUDS FOR PARTIALLY SUBMERGED MODELS

by

Paul Stoiber
A Thesis
Submitted to the
Graduate Faculty
of
George Mason University
in Partial Fulfillment of
The Requirements for the Degree
of
Master of Science
Civil, Environmental, and Infrastructure Engineering

Committee:

_____ Dr. David Lattanzi, Thesis Director
_____ Dr. Viviana Maggioni, Committee Member
_____ Dr. Girum Urgessa, Committee Member
_____ Dr. Elise Miller-Hooks, Interim Department
Chair

Date: _____ April 14th, 2023 _____

Spring Semester 2023
George Mason University
Fairfax, VA

Accuracy Analysis of Photogrammetrically Derived Point Clouds for Partially
Submerged Models

A Thesis submitted in partial fulfillment of the requirements for the degree of Master of
Science at George Mason University

by

Paul Stoiber
Bachelor of Science
California State Polytechnic University, Pomona, 2019

Director: David Lattanzi, Associate Professor
College of Engineering and Computing

Spring Semester 2023
George Mason University
Fairfax, VA

Copyright 2023 Paul Stoiber
All Rights Reserved

DEDICATION

No dedication included.

ACKNOWLEDGEMENTS

I would like to thank the many friends and family members that supported me during my graduate studies. I would also like to thank my advisor Dr. David Lattanzi and my committee advisors, Dr. Viviana Maggioni and Dr. Girum Urgessa for providing exceptional feedback and the creative liberties to shape this research to how I wanted it.

TABLE OF CONTENTS

	Page
List of Tables	vii
List of Figures	viii
List of Equations	ix
List of Abbreviations	x
Abstract	xi
Chapter One - Introduction	1
Section One – Summary of Previous Research.....	1
Section Two – Prior Work	4
Section Three – Current State of the Art and Contributions of This Research Effort ..	11
Chapter Two – Materials and Methods.....	13
Section One – Benchmark Ship Model Design.....	14
Section Two – Experimental Test Setup.....	18
Section Three – Experimental Data Collection.....	19
Section Four – 3D Point Cloud Generation	22
Section Five – Point Cloud Error Measurement	31
Chapter Three – Results.....	33
Section One – Differences in Model Dimension Accuracy	33
Section Two – Differences in Model Resolution	40
Section Three – Comparison of Model Dimensions	41
Section Four – Effects of Reflection on Model Generation.....	42
Chapter Four – Discussions and conclusions.....	45
Section One – Limitations.....	46
Section Two – Future Work	50
Appendix.....	52
Appendix A	52
Appendix B	54

References..... 55

LIST OF TABLES

Table	Page
Table 1. Median horizontal and vertical uncertainties in control points for unsubmerged model. Values are represented in millimeters.	25
Table 2. Median horizontal and vertical uncertainties in control points for unsubmerged portion of the fused model. Values are represented in millimeters.	28
Table 3. Median horizontal and vertical uncertainties in control points for submerged portion of the fused model. Values are represented in millimeters.	29
Table 4. Approximate differences in distance between the reference unsubmerged and compared partially submerged ship model. All values are represented in millimeters. ...	35
Table 5. Comparison of differences in distance between the reference unsubmerged and compared partially submerged ship model at the component level.	37
Table 6. Comparison of differences in dimensions used for the design of the model and the associated dimensions on the reference and fused models. All values are represented in millimeters.	42
Table 7. 3D coordinates of the annotated ship model part 1 taken from Autodesk Inventor. Units are in inches.	52
Table 8. 3D coordinates of the annotated ship model part 2 taken from Autodesk Inventor. Units are in inches.	53

LIST OF FIGURES

Figure	Page
Figure 1. CAD model with annotated control points.....	16
Figure 2. Example of model's paint finish.....	18
Figure 3. Example of image taken for unsubmerged model.	21
Figure 4. Example of video capture taken for partially submerged model.....	21
Figure 5. Processed 3D mesh of the unsubmerged model with registered camera stations for each image.	27
Figure 6. Processed 3D mesh of the top portion of the partially submerged model with registered camera stations for each image (top). Processed 3D mesh of the bottom portion of the partially submerged model with registered camera stations for each image (bottom)	30
Figure 7. Merged partially submerged ship model. Top figure shows before trimming. Bottom figure shows after trimming.....	31
Figure 8. Cloud to cloud comparison of unsubmerged ship model (reference) to merged partially submerged ship model (compared).....	33
Figure 9. Histogram of difference in absolute distances between the reference unsubmerged and compared partially submerged ship model. The grey line associates the histogram to a Gaussian distribution. Intensity values are scaled with blue being smaller differences in distance and green being larger differences in distance.....	36
Figure 10. Cloud to cloud comparison for the X dimension. Intensity values are scaled with green having smaller differences in distance and red having larger differences in distance.	38
Figure 11. Cloud to cloud comparison for the Y dimension. Intensity values are scaled with green having smaller differences in distance and red having larger differences in distance.	39
Figure 12. Cloud to cloud comparison for the Z dimension. Intensity values are scaled with green having smaller differences in distance and red having larger differences in distance.	40
Figure 13. Point cloud generated for the ship model above the water's surface.	43
Figure 14. Point cloud generated for the ship model above the water's surface compared to the reference model. This view is from the back of the model.....	44
Figure 15. Comparison of control point picking at different angles of image collection.	48

LIST OF EQUATIONS

Equation	Page
Equation 1	23
Equation 2	24
Equation 3	24
Equation 4	24

LIST OF ABBREVIATIONS

Polylactic Acid.....	PLA
Unmanned Aerial System	UAS
Unmanned Underwater Vehicle.....	UUV
Autonomous Underwater Vehicle.....	AUV
Computer-aided Design	CAD
Frames per Second.....	FPS
Simultaneous Localization and Mapping.....	SLAM
Structure From Motion	SFM
Extended Kalman Filter	EKF
Light Detection and Ranging	LiDAR
Red, Green, and Blue	RGB
Global Navigation Satellite System.....	GNSS
Digital Single Lens Reflex.....	DSLR
Dots per Inch.....	DPI
Root Mean Square.....	RMS
Global Positioning System.....	GPS
American Society's for Photogrammetry and Remote Sensing	ASPRS

ABSTRACT

ACCURACY ANALYSIS OF PHOTOGRAMMETRICALLY DERIVED POINT CLOUDS FOR PARTIALLY SUBMERGED MODELS

Paul Stoiber, M.S.

George Mason University, 2023

Thesis Director: Dr. David Lattanzi

There are many marine applications for 3D reconstruction ranging from the analysis of coastal erosion and bathymetric mapping using LiDAR to assisting in the structural health assessment of ships using photogrammetrically derived 3D models. As the quantity of data in all sectors of the global economy continue to grow, the historic methods of accomplishing activities such as structural inspections of ships must be succeeded by methods that cost less, save time, and provide for a safer work environment. The benefits from incorporating photogrammetrically derived 3D models can then clearly be seen when performing inspections on ships with the cost of Unmanned Aerial Systems (UAS), Unmanned Underwater Vehicles (UUV), and mounted camera systems replacing the cost of mobilizing equipment, reducing time to complete a task, and reducing the risks of in-person inspection. This study aimed to find out how accuracy was affected by merging two sets of photogrammetrically derived point

cloud data that were not collected simultaneously, both above and below the water surface. Due to phenomena such as Snell's law and barrel distortion, the image data and resulting 3D model can experience a decrease in accuracy to the real-world dimensions of a model in underwater sections compared to above water sections. This problem space has been harder to evaluate in prior work because of the typical subjects of partially submerged 3D models being large in scale, such as ships or caves, which results in non-exhaustive attempts to establish reference and control in complex physical environments. To evaluate the impacts of these distortions, a new benchmark 3D model representative of a ship's structural hull was designed, fabricated, and tested. This benchmark structure incorporated a uniform coordinate system based on target points along the surface of the hull shape, providing a basis for universal 3D reconstruction error. The impact of partial submersion on reconstruction accuracy was determined by comparing a fused model derived from a partially submerged benchmark model to a ground truth representation of the benchmark model that was unsubmerged. The results show that the absolute distance between the reference and fused model was less than 2 millimeters on average, but the maximum distances between the two models reached up to approximately 34 millimeters because of distortion caused by the water's surface during 3D model generation. Future efforts should include the application of a benchmark uniform coordinate system on physical features of a greater scale. Additionally, the development of 3D model survey quality standards independent from a geospatial reference system is a critical future work opportunity. This would allow researchers to assess how the level of accuracy captured during one surveying effort compare to the level of accuracy in a subsequent survey.

CHAPTER ONE - INTRODUCTION

Section One – Summary of Previous Research

The fact that marine engineering continues to play a critical role in the progress of globalized industries is understated. The United Nations Conference on Trade and Development (UNCTAD) discussed in their 2022 review of maritime transport that, “ships carry over 80% of volume of global trade,” with supply shortages of goods and other global factors continuing to impact maritime logistics. As seen during the COVID-19 pandemic, supply chain strains caused in part by the interruption of maritime freight transport services resulted in industries having limited to no access of basic goods and materials to integrate in their final products. Given their critical role in the global supply chain, the practice of performing routine maintenance and damage assessment of marine vessels is readily apparent. In order to improve these inspections and make them more repeatable and quantitative, methods to evaluate marine infrastructure continue to transition from visual inspections done by a person to more automated data collection strategies, such as through robotic systems. This change comes, in part, because of the visual inspection approach not being exhaustive or quantitative, resulting in inconsistent and inaccurate inspection results. Teams of robots employing a collection of remote imaging sensors to create a photorealistic and quantitative 3D model of a structure offers

a compelling alternative to conventional practice, though technical challenges must be addressed prior to practical implementation.

The capabilities of remote sensing have already enhanced the field of data collection in a diversity of research areas and industries (Navalgund et al.). Typically, remote sensing is used to create 3D reconstructions of topographic features and manmade structures. The 3D reconstructions are comprised of millions of 3D points collected using Light Detection and Ranging (LiDAR), photogrammetric collection methods, or a combination of both. LiDAR utilizes lasers at specific wavelengths and an accompanying sensor to record the reflected information of surfaces in a scanned scene. The location of the reflected information is determined by using the time it takes the laser to be emitted, reflected from a surface, and returned to the sensor. It is plugged into a formula to find the distance of a reflected surface from the sensor. The location of thousands to millions of points per second populate a 3D coordinate space to create the 3D model (Mikhail et al. 345). LiDAR scans can be taken from multiple stationary survey points and subsequently be merged into one 3D model during the data processing phase or be mounted on a mobile platform such as a UAS or UUV and merge the scans together during collection using methods such as structure from motion (SFM) (Palomer et al.). SFM uses preliminary data such as digital images and LiDAR point clouds as rough estimates for location of 3D features and then improves on each location using an iterative approach with each subsequent image or scan that is co-registered (Ding et al.).

Alternatively, 3D models can be created with large collections of images using photogrammetric resection and intersection methods. Images can be taken from typical

compact digital cameras or more professional digital cameras mounted on UASs or UUVs. When multiple images of the same physical feature are taken from different angles, the resection method determines the position and orientation of images relative to each other. After resection, 3D points can be calculated to form the 3D model when the same physical point is seen across 2 or more images (Mikhail et al. 107). The building 3D models using images from a compact digital camera was the examined method for this thesis.

The technique of extracting valuable information from the scanning of 3D features with LiDAR or SFM to construct digital elevation models for infrastructure projects has helped to reduce the time required to produce project planning data that would have taken far longer with a conventional topographic survey (Józków et al.). The data available from images when analyzed with photogrammetric workflows have helped to visualize the differences in a geological feature such as erosion in a shoreline over a large span of time or sudden changes due to landslides and hurricanes (Brock et al.). The application of photogrammetry in creating 3D models for features of interest continues to be improved and considered an acceptable cost saving alternative to LiDAR technologies, notwithstanding the possible differences in resolution (Mora et al.).

However, the marine environment poses several key challenges such as developing methods to merge 3D models of the same physical feature when portions are above and below the water's surface (Nocerino et al.). In the process of developing these alternative methods of merging 3D models of partially submerged objects, the challenge of quantifying the error seen in fused models is encountered. The challenge then becomes

determining what external factors are contributing to the fused model's error. When using a camera to capture images that can later be used in reconstruction, factors such as the distance from the sensor to the feature, light levels in the scene, and turbidity of the water contributes to poor resolution in images and, as a result, lead to poor reconstruction (Church et al.). Other factors such as how the camera's optics capture data underwater may contribute to poor reconstruction as well due to distortion across the image plane (Menna et al.).

This thesis seeks to develop a consistent approach to error analysis for 3D reconstructions performed in marine environments, particularly when imaging occurs both above and below the waterline.

Section Two – Prior Work

Initial review of the existing research shows that using photogrammetrically derived point clouds alongside other surveying methods to evaluate differences in accuracy has been investigated in other areas of remote sensing. One example is seen in the work of Mora, et al. where points clouds of construction stockpiles were derived from 3 different photogrammetry software packages and compared against a terrestrial laser scan of the stockpiles as a reference. The different point clouds were referenced to a common coordinate system by using ground control points visible in all 3D models of the stockpiles and assigning 3D coordinates that were collected from a Global Navigation Satellite System (GNSS) survey. The primary research questions of Mora, et al. identified the difference in accuracy of volumetric calculations and height values of the stockpiles between the laser scan reference model and the 3 alternative photogrammetrically derived

point cloud models. Their research showed that overall volumetric differences from the reference had an error of approximately 2 percent for the photogrammetric point clouds. When the comparison was subdivided down to the individual stockpile level, a range of errors from 0.9 to 6.5 percent was seen in the volume derived from the photogrammetric point clouds based on the software used. The comparison of height values between the reference model and photogrammetric point clouds was shown to have an error of 3 percent overall when all stockpiles were considered. A range of errors from 0.9 to 4.7 percent was seen when differences in height values of individual stockpiles were evaluated.

The use of RGB cameras to map underwater environments continues to be a topic of developing research. A sample of the application for this technology can be seen in the work of Palomer, et al., where the use of Simultaneous Localization and Mapping (SLAM) along with three methods for determining the position of the autonomous underwater vehicle (AUV) to construct and refine point clouds of a submerged structure was investigated. The feature of interest for the study was a set of interconnected PVC pipes and valves. A laser scanner developed by the group was the equipment used for data collection in the controlled water tank experiment setting. In order to recreate the submerged structure as a representative point cloud, the three methods used for SLAM were the following: dead reckoning approach, extended Kalman filter (EKF) SLAM approach, structure from motion (SFM) approach. In each condition of their experiment, the laser scanner mounted on the AUV obtained a 3D reconstruction at stationary points around the PVC structure by using travel time information from the laser back to the

camera. A dead reckoning approach involved the full reconstruction of structure by using results from navigational sensors on the AUV to designate the camera stations of the scans without any adjustments incorporated from knowledge of previous scans.

Alternatively, the EKF SLAM approach utilized 3D reconstructions from previous locations along the AUV's travel path to improve the navigational sensor's solution for position of the AUV and, subsequently, location of the current 3D scan to incorporate into the developing model. The SFM approach involved the use of an open source solution to improve the position of the AUV provided by navigational sensors to merge each 3D scan from the stationary locations along the travel path to produce the final model of the structure. The results from their experiments involved a limitation of mapping an entire 360 degree view of the structure due to size restrictions of the water tank. Clear differences in the PVC structure could be seen between the dead reckoning approach and the remaining two approaches since features such as the valves along the pipes were poorly aligned in the former approach. The focus of the work by Palomer, et al. was on improving the alignment of 3D scans to produce the final merged point cloud by evaluating how the location of the AUV and mounted laser scanner could be refined using a SFM approach and an EKF approach compared to the resulting point cloud from a dead reckoning approach. Palomer, et al. presented less of a focus on the dimensional accuracy of the final point cloud models that were created.

Regarding the fusion of multiple point clouds, the investigation done by Church, et al. into the fusion of different sensing modalities such as acoustic and laser scanning for the same submerged object evaluated how environmental conditions impacted model

reconstruction accuracy. In their study, they utilized a laser range-gated camera and a 2D BlueView sonar system to create a hybrid imaging system. An acoustic sensor allowed data to be captured further away from the device while the laser range-gated camera could capture more textural data for the submerged object at a greater resolution. The controlled experimental setup for their work included a large scale wave flume that had the option to control the level of turbidity in the water. Their imaging system was used to collect data in the flume of a target board at selected distances and turbidity levels. The resulting images produced from their work showed the capability in terms of distance from sensor that some detail could still be made out for the target board. The focus for Church, et al. was on developing a hybrid system that could leverage the benefits of both acoustic imaging and laser range gated sensors. However, there was no discussion on any losses of dimensional accuracy that were created from the fusion of the two datasets of remote sensing information.

From the work done in Palomer, et al. and Church, et al., a need for a new method to quantify dimensional accuracy of submerged features was discovered. An investigation by Appelt, et al. into how AUV travel paths could be better tracked provided details on how previous studies have compared collected data to an established reference. Their research involved the testing of a stereo camera mounted on an AUV to determine if it could be used as an acceptable alternative to more complex configurations of sensors for the purpose of localization and navigation underwater. They tested their stereo camera against three distinct types of movement patterns: linear movement, circular movement, and a free movement path. The camera collected data in calibrated and non-calibrated

trials to show how incorporating a fisheye lens model to address distortion due to underwater imaging would impact the accuracy of the recorded travel path. Their ground truth travel path was captured with an above water surface tracking system. Markers were placed on the housing of the stereo camera and remained above the water's surface for the tracking system to record the ground truth data during the different movement pattern trials. Each trial was compared to its corresponding ground truth path by aligning the two sets of data using AprilTags. They concluded that their stereo camera system could be used for underwater tracking applications if it was properly calibrated for an underwater environment due to the trends that the tracking paths take aligning with the trend from the identical ground truth path in the linear and circular movement patterns. Appelt, et al. set their focus on finding the best camera calibration parameters and how the stereo camera system's odometry path would compare to the identical ground truth path.

A key consideration in this work is how point cloud data can be fused when a physical feature crosses the open air to water medium. A thorough investigation on this topic was seen in Nocerino, et al. where fused point cloud models were created for two test cases: a capsized ship using data collected from above and below the water surface, and cave walls of a semi-submerged space using a stereo configured camera system for simultaneous video collection. In the test case of the capsized ship, a digital single lens reflex (DSLR) camera was used to collect two separate image sets that were used to photogrammetrically derive separate halves of the ship for their complete survey. One benefit to using a DSLR was the ability to interchange lenses depending on which media they were evaluating. A 35 millimeter focal length lens was used during their above the

water survey and a 24 millimeter lens was used underwater. The decision to utilize two different lenses for the two media was documented in Menna, et al. to address the radial distortions when the camera was used to collect data underwater. Nocerino, et al. utilized a collection of white circular targets and 3 meter long calibrated rods across the submerged and unsubmerged portions of the ship to construct their reference frame. The calibrated rods purposes were twofold: provide a known measurement in an image to give a sense of scale and serve as a coupled reference with specialized targets at each end. Specialized targets were visible in each photogrammetric model with a known distance between them which were used to bring the two models together to make the final merged survey of the ship. The second test case developed an alternative method for acquiring image data above and below the water surface to map a partially submerged environment. In their stereo camera setup, two GoPro cameras were calibrated to collect videos of cave walls that were used in the development of the photogrammetric model of the scene. Since there was still a possibility of radial distortion in the data taken from the video, the camera system used an assumption of fisheye lens behavior for how images were captured on the image sensor for the above the water set and a pinhole behavior for images taken below the water. From their efforts to determine the relationship of GoPro videos with respect to each camera, their study developed an algorithm to synchronize the data using visual and audio markers that were shared among the two sets. After synchronization, the photogrammetric model for the partially submerged cave was constructed. To evaluate the accuracy of their method, rods were mounted along the wall of the cave spanning across both media.

The research conducted in the current paper sought to build upon the work done in evaluating accuracy that Mora, et al. published with the added complexity of a photogrammetrically derived model utilizing data from a physical feature crossing a water media. Research performed by Church, et al. provided valuable insight on acceptable distances for the ship model from the camera and was incorporated in this research's experimental setup. Then, following a similar methodology to Appelt, et al. with some alterations, the concept of a fixed truth coordinate system was then implemented into this experiment's approach with screws in a 3D printed model that would act as tie and control points when the image data was brought into the photogrammetry software. Finally, the work of Nocerino, et al. helped to define an experiment test case by inspiring the creation of a ship model that was small enough to test in an indoor laboratory water tank.

After the analysis of the test data collected for this thesis, some research was done to see if there had been any organizations that created metrics to categorize the survey quality done for 3D models. The intention was to find a classification system that provided ranges for horizontal and vertical accuracies to distinguish higher accuracy surveys from lower accuracy surveys. The classification system that came the closest to the criteria for this research was the American Society's for Photogrammetry and Remote Sensing (ASPRS) Accuracy Standards for Digital Geospatial data. However, this accuracy standard relies on ground truth data being collected with an alternative method, such as Global Positioning System (GPS) control points taken across an imaged project boundary. Follow on research can be done in establishing a comparable survey quality

classification system for 3D features that are independent from a geospatial coordinate system. The benefit of creating this form of classification would not only provide a method to standardize the surveys performed on features such as marine ships, but also could lead to improvements in the way photogrammetric software process and categorize the resulting triangulation solutions in submerged feature datasets.

Section Three – Current State of the Art and Contributions of This Research Effort

While there is a significant body of research into optimizing the quality of 3D reconstructions, the current state of the art does not address how the accuracy of a 3D model is impacted when scans from partially submerged models are fused together. The current state of the art does show how point cloud merging underwater and across the water's surface is performed, but there are limited instances where prior work discussed the possibilities of deriving accurate measurements from the final 3D model in their work. Moreover, there is a lack of rigorous experimental design work dedicated to estimating error in 3D model reconstructions, particularly in complex scenarios such as are present in the maritime environment.

This research effort aims to develop experimental methods for quantifying 3D reconstruction accuracy, followed by an assessment of model accuracy after the fusion of submerged and unsubmerged point clouds generated from photogrammetric workflows. The experimental method is based on comparing point clouds of a 3D model designed to be a generalized version of the hull of a ship with black screws mounted across the model to establish a local coordinate system to easily align the unsubmerged and fused point clouds and perform an error comparison. Setting the screws as control points within the

model ensures that the coordinate system does not change based on external factors that may have occurred with removable control points or synchronization of collected data seen in prior work. The screws maintaining the same location allows for error estimates to be made by evaluating identical points on the model and the distance a point has translated from an acceptable reference. The analysis of the fused 3D model was achieved by utilizing this experimental apparatus to compare a fused model with a ground truth reconstruction that was entirely unsubmerged. The contributions of this research are valuable in multiple fields such as forensic analysis or damage assessment modeling and, as mentioned previously, assisting routine maintenance operations in marine structures and vessels. If a surveyor can model a partially submerged object and have confidence in the accuracy of the merged model, it can be used in quantitative life-cycle assessments. Additionally, using robots (UASs/UUVs) to create a 3D reconstruction and then assessing the model in an office setting would reduce costs incurred for underwater fieldwork and provide a safer environment for the surveyor to conduct their analyses. Another field that could benefit from this is companies involved in the removal of capsized vessels. If the merged model is created with a high degree of confidence in its dimensions, it could possibly be used for cost estimation of the removal job when quantities such as cost for cutting and removing a certain cubic foot of material is known.

CHAPTER TWO – MATERIALS AND METHODS

The research performed in this thesis evaluated differences in the accuracy of dimensions for partially submerged models using the materials listed and followed the data collection plan stated below. Additionally, a discussion on the theory behind how the chosen photogrammetric software determined point cloud location data was included to share how image data was used to create the 3D information and clarify the process from data collection to the final cloud to cloud comparison. For this experiment to be executed, the planned course of action involved the following: decide on the scope of the project in terms of size, prepare required materials and model, compose and perform data collection plan, process image data in chosen software, analyze and report on reference model to fused model comparison. The 3D model used in this thesis was the hull of a ship with black screws mounted across three surfaces designed specifically for this research experiment. The model established a local coordinate system and represented a reference frame to compare 3D reconstructions of the ship out of water and, alternatively, partially submerged without relying on reference points that could shift in position or stereo camera systems. The application of an integrated coordinate system into the physical model has not been seen in relation to evaluating accuracy in prior work.

Section One – Benchmark Ship Model Design

In contrast to prior work methods of fusing point clouds for partially submerged 3D features, this study developed a novel approach for dimensional referencing and measurement by incorporating a local coordinate system into the construction of what is referred to here as a *benchmark ship model*. A benchmark model with a fixed coordinate system allows images to be collected of the ship in a variety of environments (fully unsubmerged and partially submerged) to create 3D point clouds that can be referenced to one another without having to rely on externally mounted reference points or synchronized video data with digital markers. Screws and their associated pilot holes in the model were designed in a grid like pattern to mirror the orthogonal relationship of axes in a 3D coordinate system. The designation of 3D coordinates across the whole model instead of a handful of locations allows for more detailed alignment of point cloud data during the reference cloud to compared cloud comparison.

The design process for this experiment included prototypes of the ship model at a variety of scales. A smaller size was beneficial for initial testing to see how details from the 3D printing process would appear when the point clouds were generated. The design process helped to determine that it would be better to have an abundance of control points across the model in case the perspective captured in the camera was only able to pick up limited distinguishable points at a given camera position. Following the results of the prototype phase, the scale of the model was chosen based on critical factors such as the sensor size of the camera that would be used in data collection and the size of the experiment water tank. The final size of the model used in the experiment was 759

millimeters long, 304.8 millimeters wide, and 203.2 millimeters tall. When designing the model, holes were added to three of the four sides at set spacings of 101.6 millimeters horizontally and 50.8 millimeters vertically. Additionally, two slopes of the hull surfaces were designed with control points to evaluate if a slope that was non-vertical would cause any difference from the reference model during point cloud generation of the partially submerged model. Spacing was measured on the model from center to center of each hole. The 3D coordinate corresponded to the exterior face of the hole on each side. When control points were chosen during the point cloud model generation process, the 3D coordinates measured on the CAD model were assigned to the center point of the screw heads that were used as easily distinguishable survey markers. For the purpose of nomenclature, the left side of the ship model corresponded to the left side when facing the back side of the model that was marked with control points as well. The top left hole on the left side of the ship model that was labelled 1 in Figure 1 and was chosen as the origin for the coordinate system.

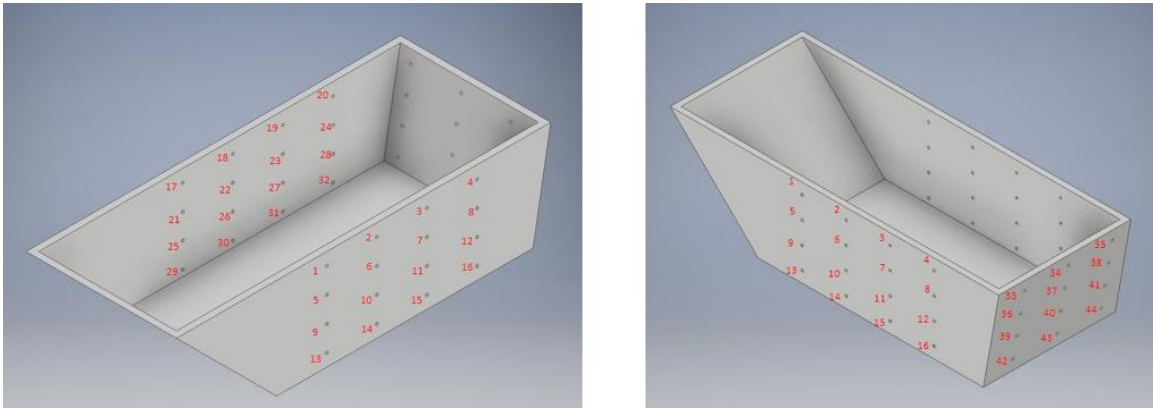


Figure 1. CAD model with annotated control points.

A table containing the 3D coordinates for the annotated ship model can be found in Appendix A. The XY plane was established on the left face of the ship. The X dimension was established horizontally across the left face increasing from the front of the ship to the back of the ship. The Y dimension represented the vertical change along the left face and increasing in value from the bottom to the top of the model. Finally, the Z axis represented the distance away from the left face of the model increasing from the right face to the left face of the model. The axis orientation is an important detail to clarify in order to make sense of the component wise breakdown in differences between the unsubmerged and partially submerged point clouds during the analysis of results.

The trial run with scaled versions of the model provided additional insight on how to best create distinguishable tie points across the model. When only the surface roughness created from the 3D printing process was evaluated, some photos were unable to align within a photogroup. A photogroup is what the photogrammetry software called a collection of photos submitted for camera position registration. Adding one color of

paint resulted in a similar outcome with some photos having an unsolved camera station in the workflow. The knowledge gained from this design process was to include multiple colors of paint and different sparsity's of points to allow the automatic tie point process to have a greater set of references to align all the photos in the workflow.

The benchmark ship model was fabricated with a Bowden Extruder type 3D printer. White PLA filament was used to create strong contrast and background separation during the point cloud generation process. The model was printed in several parts due to print bed size limitations. Due to the camera's smaller sensor size, the ship model size chosen would exhibit more detail on images than the same model at a smaller scale. The ship model was painted with three distinct colors (red, green, and blue) in order to improve the 3D reconstruction process and enhance the realism of the specimen (Figure 2).

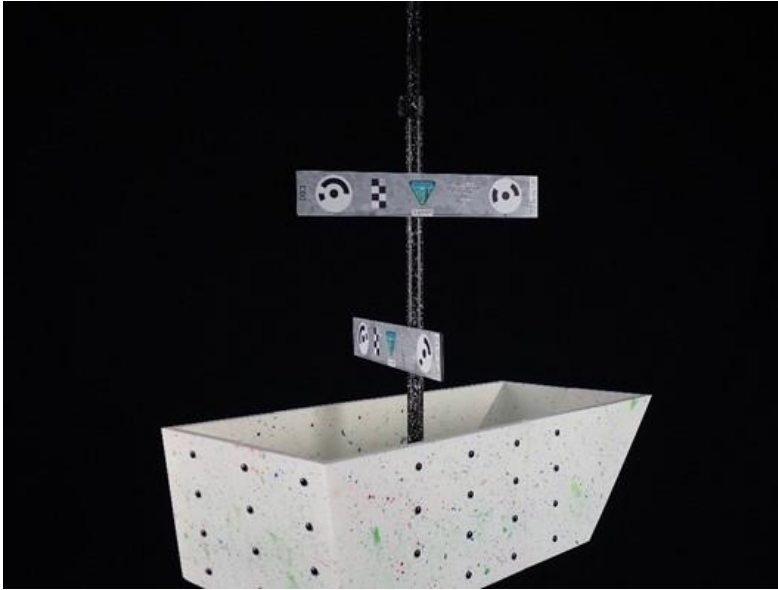


Figure 2. Example of model's paint finish.

Section Two – Experimental Test Setup

The *benchmark ship model* was suspended in a water tank for testing. The water tank used for this research was 3.5 meters in diameter and 1.2 meters deep. An overhead aluminum extrusion frame was constructed to support the ship model in the water tank. The ship model was mounted to the aluminum frame by extension of a modified electronic turntable and an extendable monopod support rod. Four studio lights were set up to control the level of illumination for the faces of the model that would be visible from the established camera station. A black backdrop was used behind the model to provide a clear contrast between the white printed ship model and other background information in the images. The centerline of the camera's frame was set up at approximately 1.2 meters away from the centerline of the model's frame.

Section Three – Experimental Data Collection

The 3D reconstructions created in these experiments utilized a stationary camera and rotating object (turntable) method of image collection and point cloud generation (Marshall et al.). Since this experiment required underwater imaging, a waterproof Olympus Tough TG-6 camera was used. The TG-6 has a 12 MP, 1/2.3-inch BSI-CMOS sensor that produces still photos at an image size of 4000x3000 pixels and video recordings at 1920 x1080 pixels at 30 fps. A separate frame was constructed and installed in the water tank to support the digital camera.

Data was collected for the ship model with an empty water tank first to create a reference point cloud for comparison of differences between the unsubmerged and partially submerged clouds. The camera was positioned at one viewpoint during each full rotation and only moved when collecting a new set of data at a different height. The turntable was used to precisely rotate the model in increments of approximately 11 degrees until an entire 360-degree view of the model was captured. The process was repeated at 6 different heights. Images were taken at a set ISO of 100 and F-stop and exposure times were automatically selected by the camera. The resulting horizontal and vertical resolution was 314 dots per inch (DPI) for each image.

Once 35 images were captured at 6 different heights for the unsubmerged ship model (210 total images), the tank was filled to a water level that left enough surface area on the exterior face of the ship model above the water surface for point cloud generation. The collection of data for the partially submerged model was done by taking videos of the ship at 4 different heights. The change in the image collection process was due to a

limitation of the camera being unable to operate remotely underwater. Additionally, the collection strategy switched from 6 heights to 4 heights to prevent the collection of duplicate images taken at the same camera location and impact the point cloud generation process. 2 heights were above the water's surface (1 high elevation view, 1 water level view) and used to create the point cloud for the above water portion of the model while 2 heights were below the water's surface (1 water level view, 1 low elevation view) and used to make the submerged portion of the model. Video frames from the 4 heights were taken for use in the photogrammetry software to build the point clouds. ISO, F-stop, and exposure times were automatically selected by the camera. The resulting horizontal and vertical resolution was 96 DPI for each video frame used in the two photogrammetric workflows.

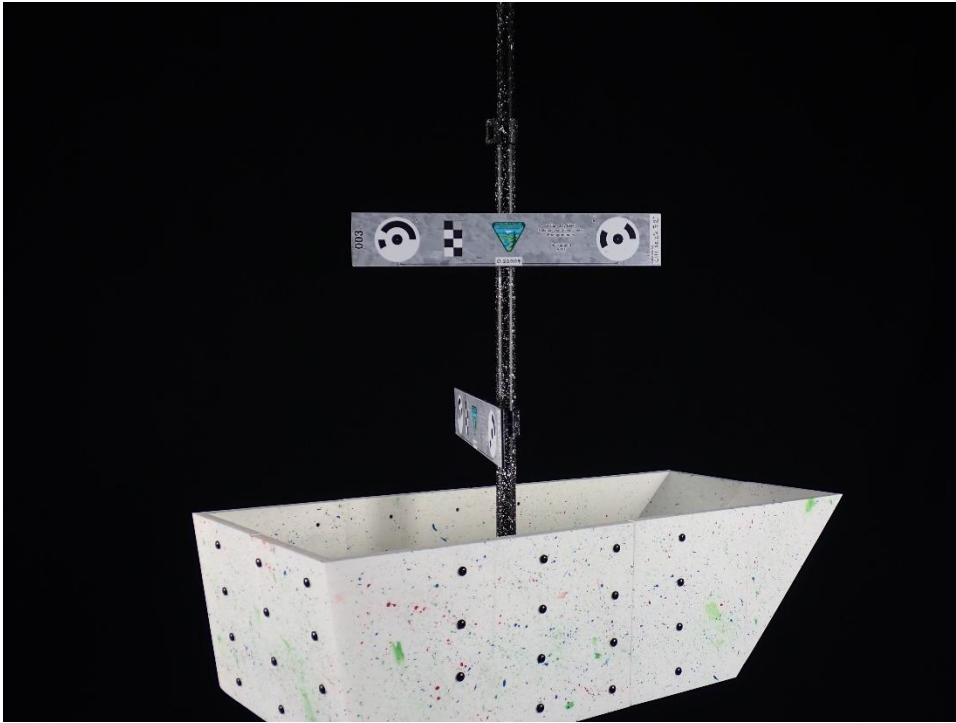


Figure 3. Example of image taken for unsubmerged model.

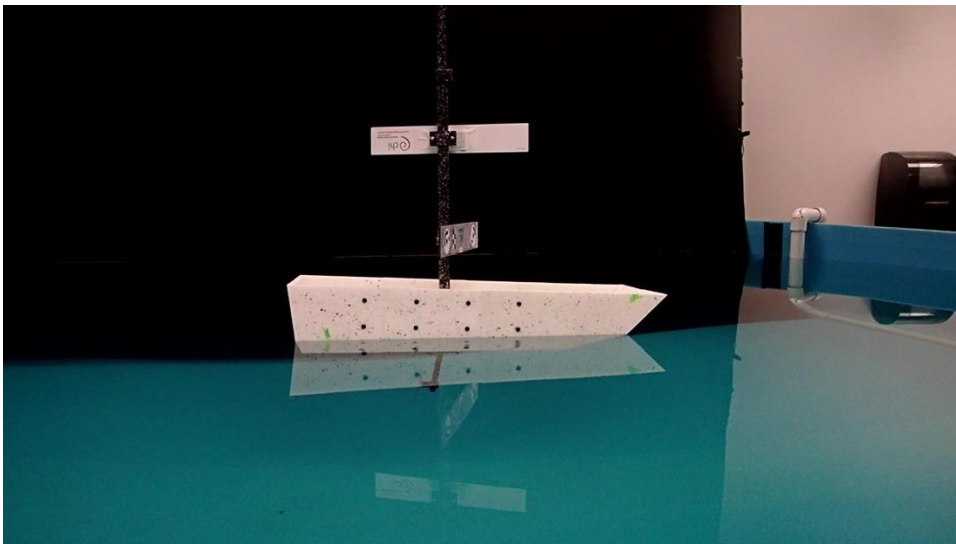


Figure 4. Example of video capture taken for partially submerged model.

Section Four – 3D Point Cloud Generation

Once the images were collected, the 3D point cloud models were generated through photogrammetric reconstruction. The photogrammetry software used in this analysis was ContextCapture. This software, developed by Bentley Systems, takes in multiple formats of imagery and point cloud data to reconstruct 3D models for use in a wide range of disciplines. For the purpose of this discussion, the generation of point clouds using imagery was highlighted. In the project workflow of ContextCapture, images were brought in as the raw data and camera parameters such as focal length were provided. Each image was then shown in the software's image viewer tool where survey points can be assigned to each image. Control points which provide a known 3D coordinate along the model were determined from the 3D model used to print the ship model and incorporated into the point selection process in the image viewer tool. The relationship between the assigned control points, camera sensor parameters, and location of identical points across multiple images is how the software calculates 3D locations for all the features of a given model space. In ContextCapture, the association between a particular feature in the image and model spaces is determined during the aerotriangulation or 3D reconstruction processing phase. As discussed in their product documentation, the method known as a bundle adjustment is applied to the image data with consideration to the 3D data provided from the control points. A bundle adjustment is the triangulation of a bundle of rays in a set of images to determine the 3D position of particular rays and exterior orientation parameters for a given image. Every image is considered a bundle of rays for this type of photogrammetry problem with an image ray

symbolizing a line that connects the image representation of a feature, perspective center of an image, and the location of the same feature in object space (Mikhail et al. 123). Image rays mathematically relate image space to object space using the collinearity equations. The form of the collinearity equations given by the ContextCapture documentation is shown below.

Equation 1

$$x = F \cdot D \left(\Pi(O \cdot R(X - C)) \right) + x_0$$

The variable x represents the 2D image space position of rays in pixels. x_0 represents the 2D location for the principal point of a given image in pixels. Uppercase X represents the 3D object space position of the associated ray in the assigned reference system for the project. C represents the 3D object space location of a given camera station in the assigned reference system. The R term represents a 3 x 3 rotation matrix that provides an initial transformation to the object space coordinates of a feature to coordinates in reference to the camera's reference system using angles that define the camera's orientation. O represents an additional 3 x 3 rotation matrix to transform the product of the previous matrix operation from coordinates referenced to the camera's orientation to coordinates in reference to how the feature is projected onto the sensor of the camera as seen in the image. The D term in Equation 1 addresses any distortion of the 2D coordinate from camera calibration parameters entered by the operator or optimal parameters found through iteration of the software's algorithm during processing. The

variable Π represents the matrix operation of converting the 3D coordinate to a 2D coordinate in the image space reference system (Equation 2).

Equation 2

$$\Pi(u, v, w) = \left(\frac{u}{w}, \frac{v}{w} \right)$$

The terms u , v , and w in Equation 2 are the X , Y , and Z coordinates derived from the rotation of the object space coordinates (Mikhail et al. 94).

Equation 3

$$\begin{bmatrix} U \\ V \\ W \end{bmatrix} = M \begin{bmatrix} X - X_L \\ Y - Y_L \\ Z - Z_L \end{bmatrix}$$

Finally, the F term is a 2×2 matrix, shown in Equation 4, that contains the focal length of the camera in pixels and adjustment factors referred to as, “the skew parameter (s) and the pixel ratio (ρ).”

Equation 4

$$F = \begin{bmatrix} f & s \\ 0 & \rho f \end{bmatrix}$$

When Equation 1 is applied on the same detected feature across multiple images, enough equations can be written to determine the location of the camera in Cartesian space, as well as the intrinsic camera parameters for each image. Every image ray in the set of images is evaluated with the collinearity equation, resulting in a 3D coordinate being determined for each distinguishable point on the images and providing the necessary information to generate a 3D reconstruction of the model (Ikeuchi 132).

For the unsubmerged point cloud model, a total of 210 images were used. A set of 11 control points from the model’s integrated coordinate system were used to digitally define the local coordinate system on the ship model. Each control point was chosen on each image where it was visible. The default horizontal and vertical accuracy of 0.3 millimeters was used for all control points. Once the control points were selected, the images were run through an aerotriangulation process where the camera stations for each image were determined using the visibility of the user defined control points and the automatically generated tie points. For this workflow, ContextCapture created 11,891 automatic tie points and resulted in a root mean square (RMS) for reprojection error of 1.04 pixels for the tie points. The 11 control points had an RMS for reprojection error of 5.85 pixels. The median horizontal and vertical uncertainties can be seen in Table 1 below. The results for the quality report showed that the average resolution in the images was 0.3 millimeters per pixel.

Table 1. Median horizontal and vertical uncertainties in control points for unsubmerged model. Values are represented in millimeters.

X axis uncertainty	0.5
Y axis uncertainty	0.1
Z axis uncertainty	0.4

Once the solution for each camera station was deemed acceptable, the images were used to make a reconstruction of the 3D scene. The reconstruction was analyzed using the extra geometric precision processing setting. Extra geometric precision is what

ContextCapture labels a tolerance of 0.5 pixel of usable information coming from the input photos during processing. Once a reconstruction was established for the image data, a 3D mesh was created to reduce the processing need for the generation of the point cloud model by establishing the reference model for the current workflow. Additionally, producing the 3D mesh allowed the quality of the photogrammetric reconstruction to be evaluated before exporting products from ContextCapture. A medium size was used in the level of detail of the 3D mesh processing settings. The final production for the unsubmerged model workflow was the creation of the point cloud model. This unsubmerged point cloud was the reference point cloud used to assess the accuracy of the fused model comparison.

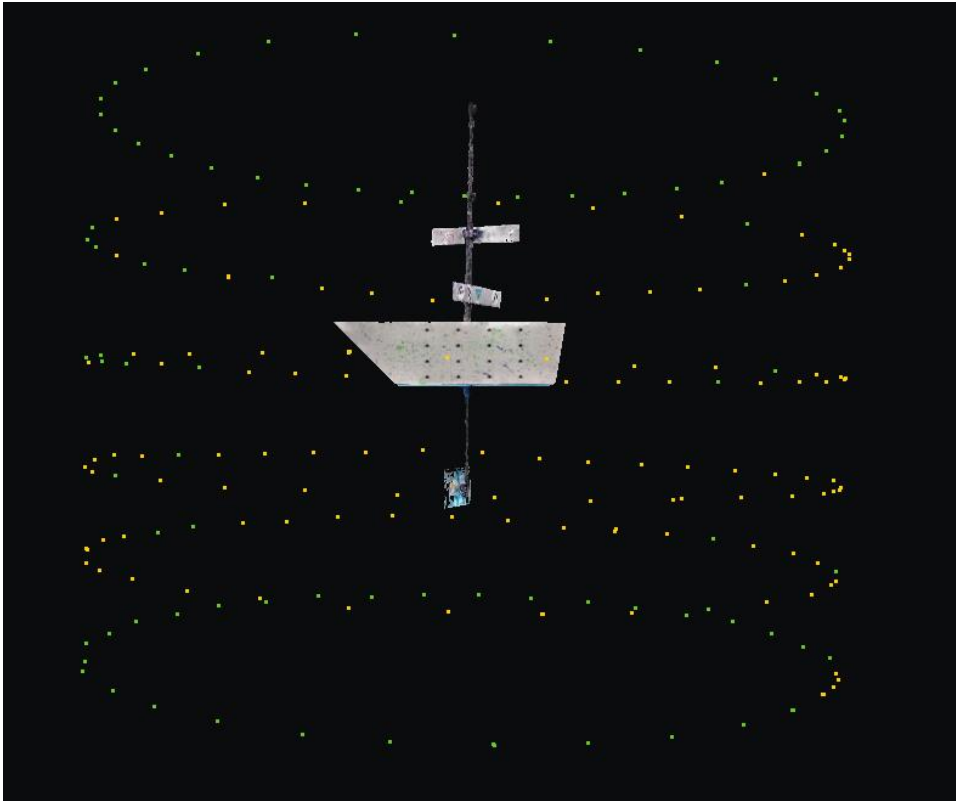


Figure 5. Processed 3D mesh of the unsubmerged model with registered camera stations for each image.

The two separate photogrammetric workflows for the fused model consisted of one reconstruction for the portion of the model that remained above the water's surface and one for the portion of the model that was submerged. For the unsubmerged portion of the partially submerged ship model, a total of 104 photos was used in the analysis. For the aerotriangulation process, 10 control points from the model's integrated coordinate system were selected to digitally define the established local coordinate system on the ship model. The default horizontal and vertical accuracy for the control points remained unchanged. Additionally, 5 user tie points were chosen to improve the calculation for all the camera stations in the 104 images. The unsubmerged portion had 2,001 automatic tie

points and resulted in an RMS for reprojection error of 0.83 pixels for the tie points. The 10 control points had an RMS for reprojection error of 1.54 pixels. The median horizontal and vertical uncertainties for this workflow can be seen in Table 2. The results for the quality report showed that the average resolution in the images was 1.1 millimeters per pixel.

Table 2. Median horizontal and vertical uncertainties in control points for unsubmerged portion of the fused model. Values are represented in millimeters.

X axis uncertainty	0.1
Y axis uncertainty	0.1
Z axis uncertainty	0.1

The reconstruction for this workflow used the ultra geometric precision processing setting. Ultra geometric precision is what ContextCapture labels a tolerance smaller than extra which uses more memory and longer computation time to represent the resolution of usable information coming from the input photos during processing. A 3D mesh was then created using a medium size level of detail within the processing settings. Finally, the point cloud for the unsubmerged portion of the ship model could be generated from the preliminary analysis.

Once the workflow for the unsubmerged portion of the model was completed, the processing for the submerged portion of the model was conducted. The analysis for this portion of the ship model used a total of 88 photos. 9 control points and 4 tie points were defined by the user for the aerotriangulation process. Once again, the default values for

the horizontal and vertical accuracy of the control points remained unchanged. The submerged portion had 1,245 automatic tie points and resulted in an RMS for reprojection error of 0.94 pixels for the tie points. The 9 control points had an RMS for reprojection error of 2.34 pixels. The median horizontal and vertical uncertainties for this workflow can be seen in Table 3. The results for the quality report showed that the average resolution in the images was 0.6 millimeters per pixel.

Table 3. Median horizontal and vertical uncertainties in control points for submerged portion of the fused model. Values are represented in millimeters.

X axis uncertainty	0.4
Y axis uncertainty	0.4
Z axis uncertainty	0.3

The reconstruction for the submerged portion used the extra geometric precision processing setting. The medium size level of detail was once again utilized to produce the 3D mesh. The point cloud for the submerged portion of the model derived from the 3D mesh of the current workflow was exported from the photogrammetry software along with the unsubmerged portion that was previously generated. Both portions of the partially submerged model were brought into the CloudCompare point cloud visualization software to be fused into one for comparison to the unsubmerged reference point cloud of the ship model.

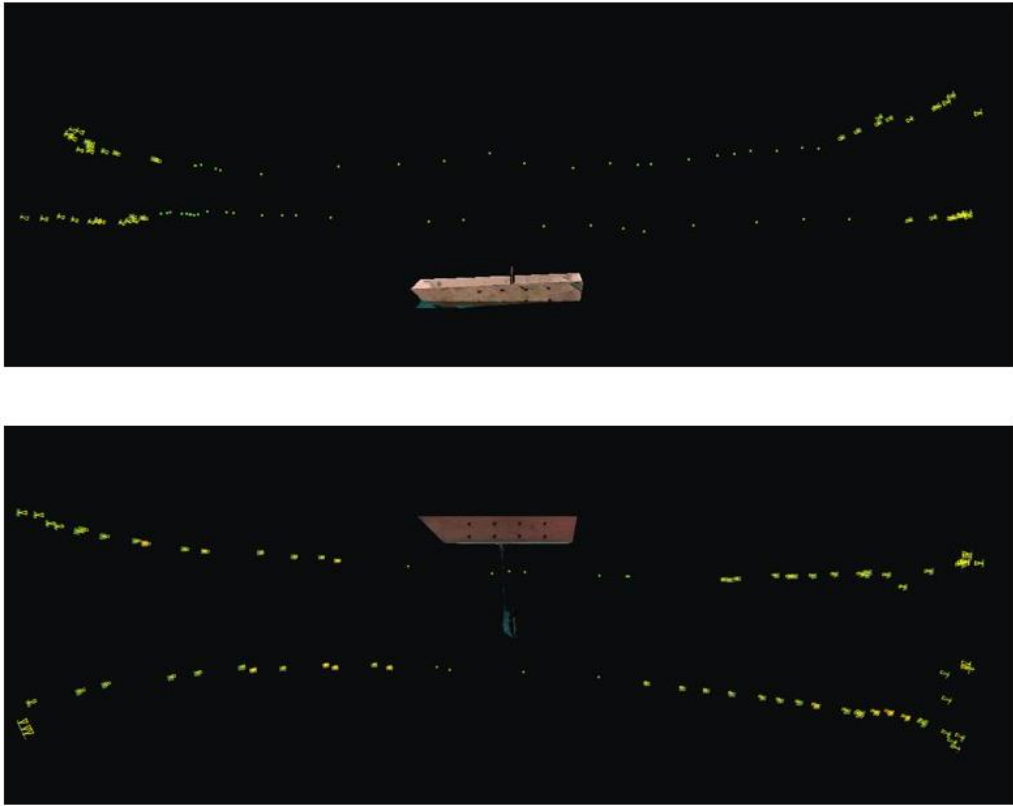


Figure 6. Processed 3D mesh of the top portion of the partially submerged model with registered camera stations for each image (top). Processed 3D mesh of the bottom portion of the partially submerged model with registered camera stations for each image (bottom)

Since both point clouds were referenced to the established local coordinate system in the ContextCapture software, the top and bottom portions of the partially submerged model were imported into CloudCompare with an acceptable rotation to allow each face of the model to be aligned with the remainder of each face in the subsequent point cloud without any alterations. In order to fuse the two points clouds, the merge capability in CloudCompare was used. The resulting merged model for the partially submerged condition can be seen below.

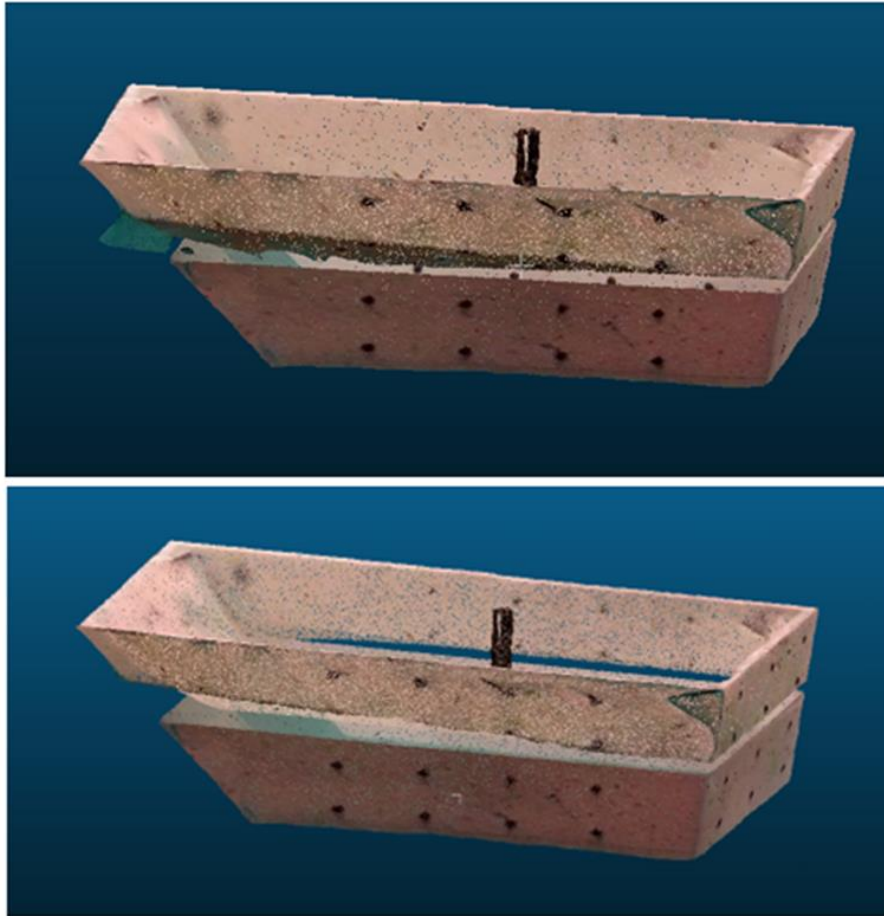


Figure 7. Merged partially submerged ship model. Top figure shows before trimming. Bottom figure shows after trimming.

Section Five – Point Cloud Error Measurement

The unsubmerged model and fused model were imported to CloudCompare and a cloud-to-cloud distance comparison was performed. The unsubmerged model was chosen as the reference point cloud and the fused model was set as the compared point cloud. Since the uniform coordinate system was previously established by the selection of

control points during the point cloud creation phase using the model's integrated coordinate system, the reference and fused models did not require any alignment adjustments. The cloud-to-cloud comparison was analyzed at an absolute 3D distance level and subsequently broken down to the X, Y, and Z components. A cloud to cloud distance comparison was chosen as an acceptable metric for accuracy since the *benchmark ship model* is the same 3D object in both the reference and fused model. When the unsubmerged model was established as the reference, any other 3D model generated through alternative workflows should result in the same model and produce cloud to cloud distances close to zero. Evaluating how the same feature differs between a reference and compared point cloud is how error measurements are made in a point wise comparison. Any cloud to cloud distance greater than zero would show that the fused model was impacted by differences in the point cloud generation process or image collection process. Additionally, the principal dimensions (length, width, and height) of the reference and fused models in relation to the true dimensions designed for the ship in the Autodesk Inventor CAD software were examined.

CHAPTER THREE – RESULTS

Section One – Differences in Model Dimension Accuracy

From the cloud-to-cloud distance comparison between the unsubmerged model and the fused model, the fused model was seen to retain accurate dimensions with an average approximate difference of 1.7 millimeters with a standard deviation of 2.9 millimeters. This accuracy was determined from a Gaussian distribution evaluation of all the absolute distances between the fused and reference point clouds. The greatest differences, as seen in the figure below, were at the transition surface between the submerged and unsubmerged portions of the ship model.

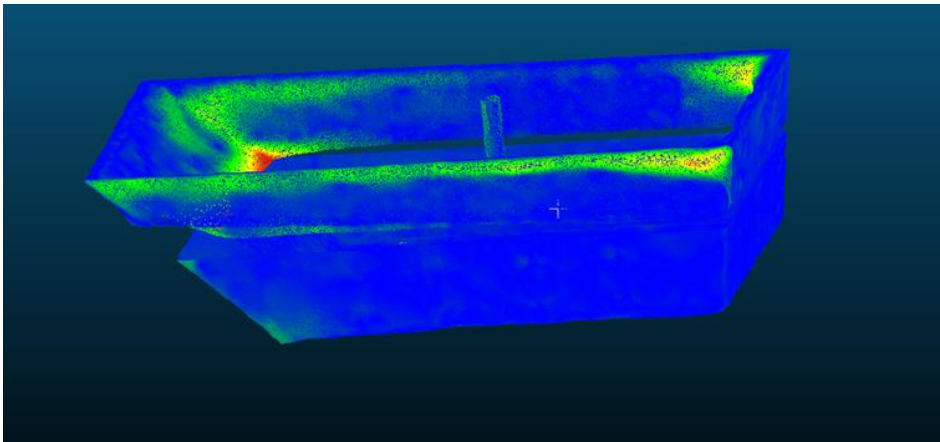


Figure 8. Cloud to cloud comparison of unsubmerged ship model (reference) to merged partially submerged ship model (compared).

Figure 8 represents a visual interpretation of the difference in approximate absolute distances between the reference and compared point clouds. Intensity values are scaled with blue having smaller differences in distance and red having larger differences in distance. The absolute cloud to cloud distance showed a significant difference between the average distance of 1.7 millimeters and maximum distance of 33.9 millimeters primarily where the model interfaced with the water's surface. The difference between the average absolute distance and maximum absolute distance provided a numerical representation that the Gaussian distribution was not a well fitted distribution for the cloud to cloud distances dataset as seen in Figure 9. Additional locations across the model where larger cloud to cloud distances were observed along the top edge of the exterior (hull) surface and interior surfaces of the model. The primary reason for the greatest errors was due to reflections from the water's surface causing the points of the interior surface of the model to be placed in incorrect locations, or locations that are translated from their proper location on the model's surface, during point cloud generation. For less significant differences in the cloud to cloud distances such as the top edge of the left surface, differences could be attributed to the angle of collection limitation for images seen when comparing Figure 6 to Figure 5 due to the configuration of the lab space. Since there were less images to extract data from to delineate between the left surface and top of the model, the software generated the top edge with less accuracy than other regions of the unsubmerged portion of the fused model during reconstruction. Similar to the top edge of the left surface, some interior surfaces of the

model showed less significant differences due to the angle of collection limitation for images. When comparing the surfaces on the side of the ship to the sloped surface on the back of the ship, no significant difference in distance between the reference and fused model was observed. Results from the absolute cloud to cloud distance comparison can be seen in Table 4.

Table 4. Approximate differences in distance between the reference unsubmerged and compared partially submerged ship model. All values are represented in millimeters.

Minimum Distance	0
Maximum Distance	33.9
Average Distance	1.7
Standard Deviation	2.9

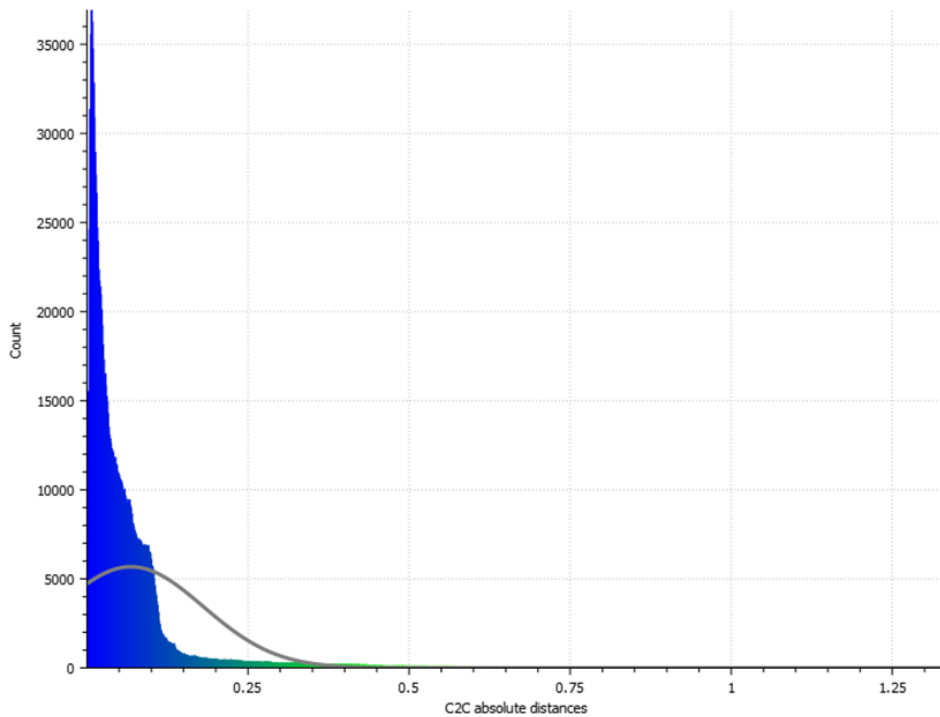


Figure 9. Histogram of difference in absolute distances between the reference unsubmerged and compared partially submerged ship model. The grey line associates the histogram to a Gaussian distribution. Intensity values are scaled with blue being smaller differences in distance and green being larger differences in distance.

Following the alignment of the reference model to the fused model, a gap in the fused model was observed. This gap was the result of point cloud data being trimmed from the top and bottom point cloud models generated in the two separate photogrammetric workflows and a lack of meaningful data near the water line. Trimming was performed in order to reduce some impacts of reflection on the model caused by the water's surface and reduce the likelihood that points would be created that incorrectly represent locations of the model in 3D space. The size of the gap was the result of how the water line was positioned across the model's exterior surface that would impact a proper representation of the model. The trimming of the unsubmerged portion of the

fused model and the gap created by the water line did not contribute to larger values in the cloud to cloud distance comparison because the reference model did not have an equivalent 3D point in the fused model to evaluate. This was shown in Figure 8 with the gap observed in the fused model not having intensity values in the cloud to cloud distance comparison. The effects of surface reflection on point cloud generation are shown in section 3.4.

Along the X dimension, there was a difference of 0.1 millimeters and standard deviation of 1.6 millimeters between the fused and the fully unsubmerged point cloud. The Y dimension had an average difference of 0.2 millimeters and standard deviation of 1.6 millimeters. Along the Z dimension, an average difference of 0.2 millimeters and standard deviation of 2.4 millimeters was observed. The breakdown of the differences at the component level can be seen in Table 5 below.

Table 5. Comparison of differences in distance between the reference unsubmerged and compared partially submerged ship model at the component level.

	X Component	Y Component	Z Component
Average Distance (mm)	0.1	0.2	0.2
Standard Deviation (mm)	1.6	1.6	2.4

When the X component of the cloud to cloud comparison was evaluated, the greatest differences were found in the portion of the fused model above the water's surface. Isolated areas such as the interior surface of the ship model presented differences

represented in red that were in the range of 18.5 to 28.4 millimeters. Other areas such as the interior surface for the back of the ship model visualized differences in a darker green and blue that ranged from 17.9 to 24.6 millimeters. In Figure 10 below, the submerged portion of the fused model was shown to have differences in the range of 1.9 to 4.7 millimeters.

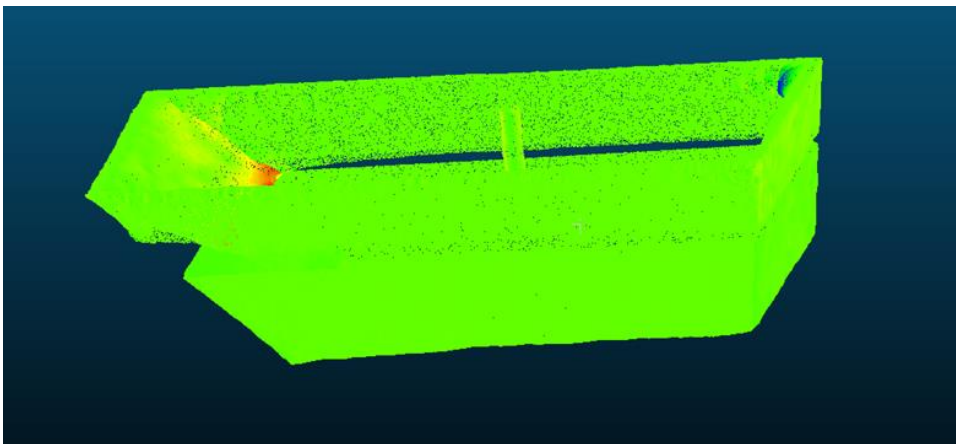


Figure 10. Cloud to cloud comparison for the X dimension. Intensity values are scaled with green having smaller differences in distance and red having larger differences in distance.

After reviewing the X component of the comparison, the Y component was inspected with the greatest differences still found in the portion of the fused model above the water's surface. Areas with the greatest difference were seen once again on the interior surface of the ship model represented in orange and red with a range of 21.6 to 31.4 millimeters. In contrast to the X component visualization, the interior surface for the back of the ship model did not show significant cloud to cloud differences that instead

ranged from 0.2 to 7.5 millimeters. In Figure 11 below, the submerged portion of the fused model was shown to have differences in the range of 0.2 to 4.6 millimeters.

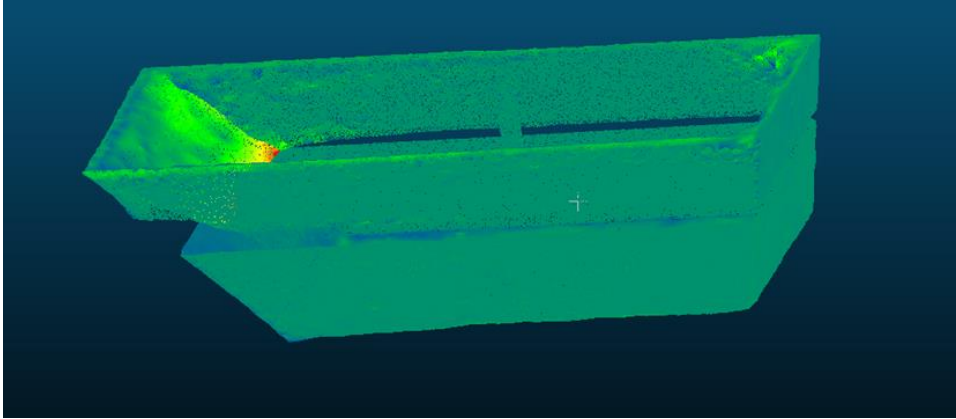


Figure 11. Cloud to cloud comparison for the Y dimension. Intensity values are scaled with green having smaller differences in distance and red having larger differences in distance.

Since the Z component presented the greatest average distance between the two point clouds compared to the previous components, it can be discerned that the Z component contributed greater weight to the absolute differences between the two sets of data having larger values. This point can be seen visually in Figure 12 because of the shift from the overall blue intensity values in Figure 8 to bright green intensity values, indicating a larger change in absolute distance since the fused model has a larger difference from the reference model at the Z component level. Additionally, in Figure 12 below, the differences exclusively in the Z dimension were visualized with the red intensity values symbolizing where the maximum difference in distance between the reference and fused models was located. Areas with red intensity values had differences

in the range of 21.3 millimeters to 32.7 millimeters. Areas with green intensity values had differences in the range of 6.1 millimeters to 12.8 millimeters.

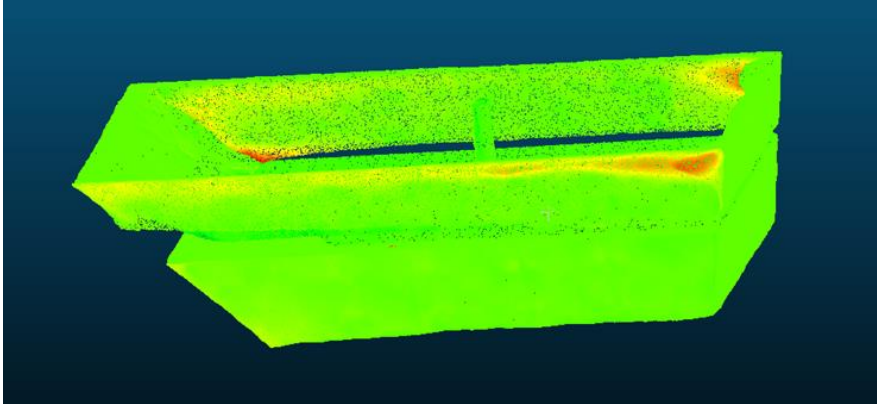


Figure 12. Cloud to cloud comparison for the Z dimension. Intensity values are scaled with green having smaller differences in distance and red having larger differences in distance.

Section Two – Differences in Model Resolution

Since the process of image collection changed between the unsubmerged and partially submerged trials, any impacts on how the resolution of the model differed were evaluated. For the unsubmerged trial, the 210 images across 6 levels of height produced a point cloud with 25,425,465 points using the processing settings reported. The unsubmerged portion of the fused model used 104 images across 2 levels of height and produced a point cloud with 520,815 points with the reported settings. Finally, the submerged portion of the fused model used 88 images across 2 levels of height and produced a point cloud with 1,071,746 points with the reported settings. The resulting sample distance in the unsubmerged model was approximately 0.2 millimeters. The

sample distance in the fused model was approximately 14.9 millimeters for the unsubmerged portion and approximately 0.9 millimeters in the submerged portion. The portion of the model that was in direct contact with the water to surface medium resulted in a gap of approximately 18.2 millimeters in the two portions of the fused model.

Some differences in resolution occurred due to the transition from still images to captures from video recordings to operate the submerged camera equipment. Since video could only be captured at 1920 x 1080 pixels versus the 4000 x 3000 pixels of still images, the smaller quantity of points observed in the fused model makes sense. Additionally, transitioning from 6 levels of height collected for the reference model at 11 degree increments resulted in significantly more data than the 4 levels of height for the partially submerged model. The coverage of the model at each height level tried to maintain the 11 degree increments set in the unsubmerged data collection process but was ultimately limited by the resolution of images captured from the recorded videos. Additionally, the limitation of access to space around the water tank prevented the camera from capturing the full 360 degree view of the model that was possible with the data collection for the reference model.

Section Three – Comparison of Model Dimensions

The point cloud models were evaluated based on how they represented the true dimensions of the ship model specified through 3D printing. A comparison of the ship models' length, width and height measurements are shown in the table below. Design measurements were found in Autodesk Inventor, the software in which the ship was

designed. Reference and fused models' measurements were found with distance tools in CloudCompare.

Table 6. Comparison of differences in dimensions used for the design of the model and the associated dimensions on the reference and fused models. All values are represented in millimeters.

	Length	Width	Height
Design Measurements	759.0	304.8	203.2
Reference Model	747.2	299.1	195.8
Fused Model	746.2	312.3	202.1

The reference and fused models had similar percent differences from the design length of 1.59 percent and 1.68 percent, respectively. A greater percentage difference was seen between the two models in the width and height dimensions. Along the width dimension of the ship, the reference model had a percent difference of 1.87 percent from the design width while the fused model produced a 2.45 percent difference. In the height dimension, the reference model had a 3.67 percent difference from the design height while the fused model's percent difference was recorded as 0.54 percent.

Section Four – Effects of Reflection on Model Generation

During the point cloud generation of the above water portion of the model, visual artifacts from the reflection of the water's surface were observed in the point cloud. These artifacts are seen in blue along the bottom edge of the front and left surfaces of the model as seen in Figure 13. The impact of analyzing the preliminary point cloud data

shown in Figure 13 resulted in some of the reflected surface still being visible in the cloud to cloud comparison prior to point cloud trimming shown in Figure 8. This artifact would have contributed to additional measurements in CloudCompare's distance comparison between the reference and fused model and resulted in redundant larger distances in Figure 9 and a shifted dataset for the average in Table 4.

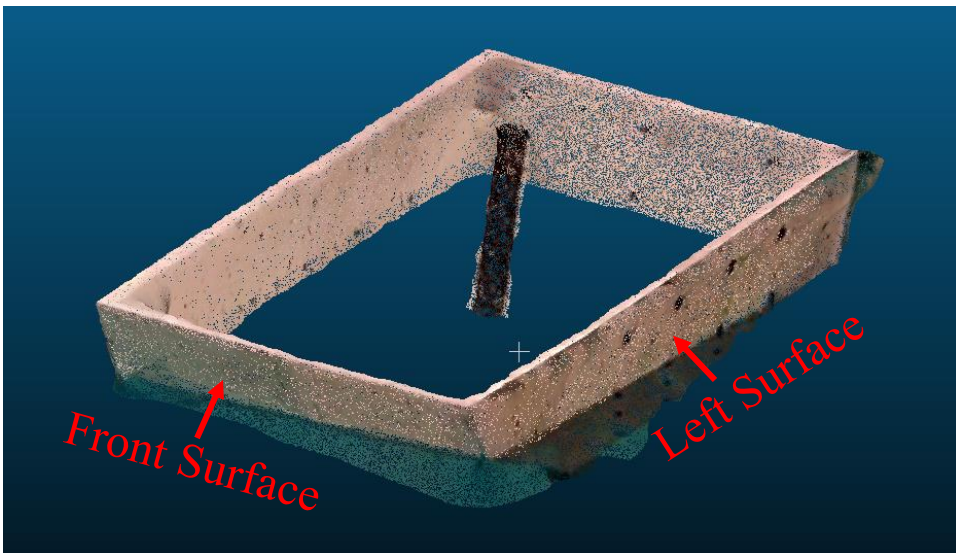


Figure 13. Point cloud generated for the ship model above the water's surface.

Due to the angle of collection for some frames taken from above the waterline, the reflection of the water behind certain edges created distortion in the edges as seen along the top edge of the left surface in Figure 13 near the back of the model.

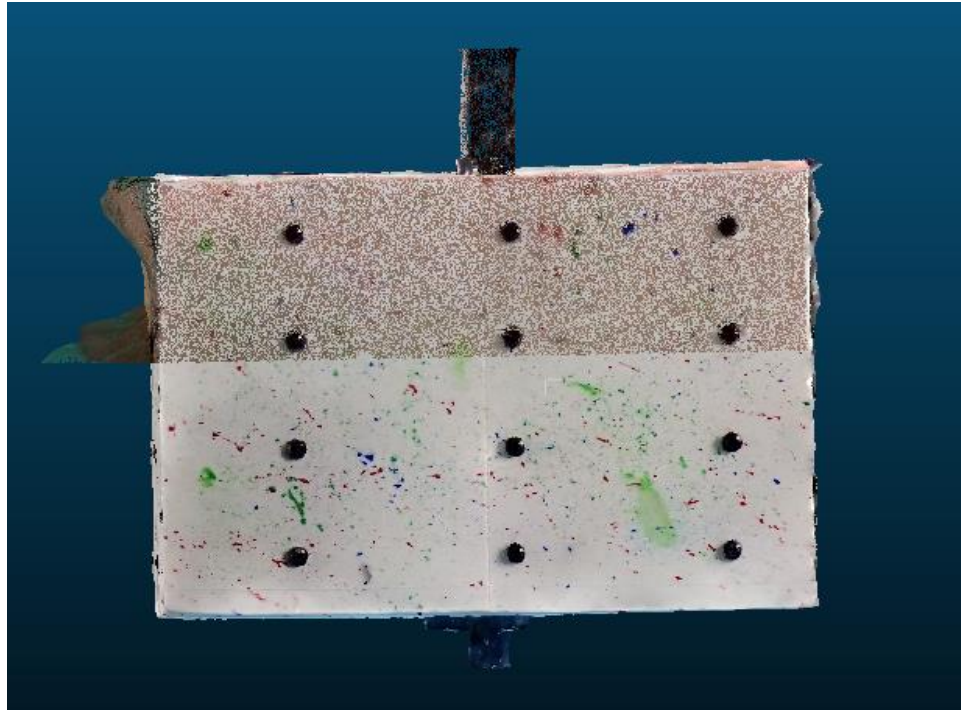


Figure 14. Point cloud generated for the ship model above the water's surface compared to the reference model. This view is from the back of the model.

Figure 14 provides an alternative view of the distortion with an overlay of the reference model. These differences in position for the edge of the model were noticeable in the cloud to cloud comparison of Figure 8 as well. Similar to the reflection of the water's surface near the front of the model, the distortion of the top edge of the fused model could have resulted in redundant larger distances in Figure 9 and a shifted dataset for the average distance in Table 4.

CHAPTER FOUR – DISCUSSIONS AND CONCLUSIONS

This study aimed to address the challenges encountered in the current state of the art with respect to unifying separate point clouds across a water's surface and evaluate if there were noticeable impacts to accuracy of the reconstructed model. It also aimed to create an experimental process for doing so through the design of a benchmark test structure. From the analysis of data captured in this laboratory setting, this research was successful in visualizing the differences in accuracy between the partially submerged and unsubmerged models using a uniform coordinate system tied to this benchmark model. This thesis provided insight on how a fused model for a partially submerged feature was affected at a quantitative and qualitative level. The results from the fused point cloud to reference point cloud comparison for the ship model showed that there was an average difference of less than 2 millimeters at the absolute difference level, however, major errors were observed at locations across the unsubmerged portion of the fused model that interfaced with the water's surface. The largest error can be seen from the difference of the maximum cloud to cloud distance of 33.9 millimeters from the average of 2 millimeters on the interior front surface of the model that was in contact with the water's surface. The next largest error can be seen on the back end of the left exterior (hull) surface with a cloud to cloud distance of 31.8 millimeters that had distortion caused by the angle of collection of the images used in the reconstruction of the unsubmerged

portion of the model. When broken down to the component level, an average difference of less than 1 millimeter was reported. The experiment performed for this research was successful in showing the smaller differences of the fused model from the reference model across multiple regions of the ship but was unsuccessful in properly addressing differences in regions where effects of reflection from the water's surface may have distorted particular features in the fused point cloud.

Section One – Limitations

After the conclusion of this study's data collection phase, details that could be further improved in future iterations of this experiment were considered. The key points that will be addressed were divided into the following categories: hardware limitations, experiment setup limitations, and optical considerations.

Due to the limitations that arose from the operation of the camera equipment when the unit was submerged, captures from video recordings done with the same camera were used to replace still images taken from a stationary camera station. This technological limitation could be removed in follow on experiments by using SD cards that have faster read and write speeds or by finding camera equipment that could be operated remotely underwater to take still images instead of relying on screen captures from a video which may suffer from motion blur.

The hardware limitation of underwater operation of the camera contributed to the reduced scope of data collection as well. During the unsubmerged model data collection process, 6 levels of height were collected to construct the reference point cloud model. Each stage was able to capture a full 360 view of the model at 11 degree increments as a

result of the controlled rotation of the electronic turntable. Conversely, the partially submerged model data collection process was only able to capture 4 levels of height with 2 being above the water's surface and 2 being below. Due to the size restrictions of the ship model, the electronic turntable could not provide highly precise controlled rotation of the model. As a result, the camera could not remain stationary, and the image data was collected using video recordings while the model remained stationary. The coverage of the model at each height level tried to maintain the 11 degree increments set in the unsubmerged data collection process but was ultimately limited by the resolution from the recorded videos. Additionally, the limitation of access to space around the water tank prevented the camera from capturing a full 360 degree view of the model. The gap in coverage can be seen when comparing Figure 5 to Figure 6. In future research efforts, this limitation could be resolved by improving the turntable assembly to accommodate the horizontal rigid motion observed with the ship model and allow the camera to remain stationary.

During the control and tie point selection processes, it became clear that the level of illumination in the underwater scene was low. The use of studio light fixtures provided a satisfactory illumination level for images above the water surface but did not provide an advantage for underwater scenes. In future investigations in a controlled experiment setting, the use of lights with enclosures that allow it to be submerged and provide additional light that can be reflected off the surfaces of the model may help to address the lower visibility issues encountered in submerged settings.

Another area of improvement in the experiment setup is the use of alternative control point markers. The use of black screws mounted on the white model provided a sharp contrast for identification of known locations on the model. Variations in dimensions such as the thickness of the screw head and the shape of the screw drive could have added some uncertainty when fine tuning the selected control points on some images based on the angle of the camera relative to the head of the screw on the model as seen in Figure 15.

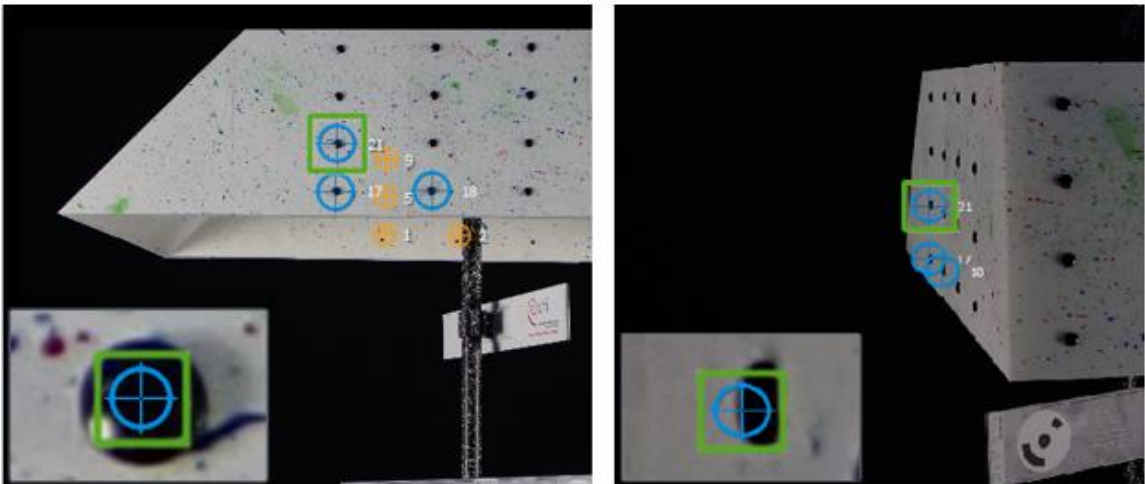


Figure 15. Comparison of control point picking at different angles of image collection.

In future research, if control point markers were identified on a model using a flatter reference surface, it would allow a more proper location for the control points to be chosen in the photogrammetric workflow. Furthermore, the addition of patterns similar to

what is found on calibration targets on the flatter reference surfaces would allow for a clearer center point on the control marker.

In the area of model improvement for future investigations, the use of alternative surface details to assist automatic tie point selection can be evaluated. The use of three distinct colors in a densely speckled finish was used because it resulted in better automatic tie point selection in preliminary testing compared to earlier sample models in this study. When photogrammetric workflows were performed on models with more sparsely spaced finishes, the camera stations for some images could not be found because a smaller collection of tie points was used with fewer correlations between images. The addition of greater surface roughness to the model than what was tested during the prototype phase may provide an added level of detail for the automatic tie point selection process to utilize and further improve the solutions for image camera stations and subsequent construction of point cloud models for accuracy comparisons.

When reviewing the quality report of the submerged portion of the model, the lens distortion caused by the difference in the refractive index between air and water was seen. This was evident by observing the difference between a zero distortion grid reference that would produce the accurate dimensional values of a feature and the identical feature shown with a different value in the grid produced from the underwater images. Although, since the model consistently remained in the center of the images, the distortion near the edge of the lens did not seem to impact how the dimensions of the submerged portion of the model were generated as observed in the minor differences between the reference point cloud and the submerged portion of the fused point cloud. As

a result, this research helps to provide evidence towards the assumptions made in Nocerino, et al. and Menna, et al. about the effects of the medium with respect to radial distortion while collecting images for subsequent photogrammetric models.

Section Two – Future Work

The discussion on the accuracy of 3D feature positions presented by this research opens many possibilities for further investigation. As mentioned in the prior work section, the search for a survey classification system that could be applied during the data analysis phase of this research presented a possibility for future work to develop a set of standards for evaluating 3D model survey quality. In addition to performing this experiment again in a controlled environment, future research could also investigate if quantitative differences between a reference and fused model would remain at the 2 millimeter level found in this research when tested on larger models or actual marine size vessels. If an experiment could be performed on a model at two different scales, the effect of the model size on model accuracy could be identified. This information could then be translated to studies evaluating actual size models in an uncontrolled environment instead of only scaled ones in a controlled environment.

Along with transitioning this method of establishing a coordinate system for a fused model from a controlled environment to an uncontrolled environment, impacts on model accuracy from variables that are harder for researchers to control should be evaluated. For example, the impact of variable tide levels across a period of time on establishing the delineation between the below water and above water surface portions of a marine vessel can be investigated. An evaluation of a ship or marine structure when the

tide levels differ may provide additional information for the generation of the fused point cloud model since the major gap in this study's fused model was the result of the water's surface level being constant. The difference in the water's surface level could provide enough reference information in the images to reconstruct a continuous surface for the partially submerged features. Other environmental factors such as turbidity and available light levels should also be studied.

APPENDIX

Appendix A

Table 7. 3D coordinates of the annotated ship model part 1 taken from Autodesk Inventor. Units are in inches.

ID	X	Y	Z
1	0	0	0
2	4	0	0
3	8	0	0
4	12	0	0
5	0	-2	0
6	4	-2	0
7	8	-2	0
8	12	-2	0
9	0	-4	0
10	4	-4	0
11	8	-4	0
12	12	-4	0
13	0	-6	0
14	4	-6	0
15	8	-6	0
16	12	-6	0
17	0	0	-12
18	4	0	-12
19	8	0	-12
20	12	0	-12
21	0	-2	-12
22	4	-2	-12

Table 8. 3D coordinates of the annotated ship model part 2 taken from Autodesk Inventor. Units are in inches.

ID	X	Y	Z
23	8	-2	-12
24	12	-2	-12
25	0	-4	-12
26	4	-4	-12
27	8	-4	-12
28	12	-4	-12
29	0	-6	-12
30	4	-6	-12
31	8	-6	-12
32	12	-6	-12
33	17.708	0.015	-2.5
34	17.708	0.015	-6.5
35	17.708	0.015	-10.5
36	17.361	-1.954	-2.5
37	17.361	-1.954	-6.5
38	17.361	-1.954	-10.5
39	17.013	-3.924	-2.5
40	17.013	-3.924	-6.5
41	17.013	-3.924	-10.5
42	16.666	-5.894	-2.5
43	16.666	-5.894	-6.5
44	16.666	-5.894	-10.5

Appendix B

The 3D model used in this research is available for future investigations as supplemental material submitted with this research effort.

REFERENCES

- Appelt, Tim, et al. "Calibration and Validation of the Intel T265 for Visual Localisation and Tracking Underwater." *The International Archives of Photogrammetry, Remote Sensing and Spatial Information Sciences* 43 (2021): 635-641.
- ASPRS Accuracy Standards for Digital Geospatial Data.*
https://www.asprs.org/a/society/divisions/pad/Accuracy/Draft_ASPRS_Accuracy_Standards_for_Digital_Geospatial_Data_PE&RS.pdf.
- Brock, John C., and Samuel J. Purkis. "The emerging role of lidar remote sensing in coastal research and resource management." *Journal of Coastal Research* 10053 (2009): 1-5.
- Bentley - Product Documentation.* Bentley Systems,
https://docs.bentley.com/LiveContent/web/ContextCapture_User_Guide_EN_PDF-v18/en/ContextCapture%20User%20Guide%20EN.pdf.
- Church, Philip, et al. "Overview of a hybrid underwater camera system." *Ocean Sensing and Monitoring VI*. Vol. 9111. SPIE, 2014.
- Ding, Li, and Gaurav Sharma. "Fusing structure from motion and lidar for dense accurate depth map estimation." *2017 IEEE international conference on acoustics, speech and signal processing (ICASSP)*. IEEE, 2017.

- Ikeuchi, Katsushi, ed. *Computer vision: A reference guide*. Cham: Springer International Publishing, 2021.
- Józków, Grzegorz, Charles Toth, and Dorota Grejner-Brzezinska. "UAS topographic mapping with velodyne LiDAR sensor." *Isprs annals of the photogrammetry, remote sensing and spatial information sciences* 3 (2016): 201.
- Kolyvas, Efthymios, et al. "Application of photogrammetry techniques for the visual assessment of vessels' cargo hold." *16th International Congress of the International Maritime Association of the Mediterranean, IMAM 2015*. 2015.
- Marshall, M. E., et al. "Automating photogrammetry for the 3d digitisation of small artefact collections." *The International Archives of Photogrammetry, Remote Sensing and Spatial Information Sciences* 42 (2019): 751-757.
- Menna, Fabio, et al. "A photogrammetric approach to survey floating and semi-submerged objects." *Videometrics, Range Imaging, and Applications XII; and Automated Visual Inspection*. Vol. 8791. SPIE, 2013.
- Mikhail, Edward M., et al. *Introduction to Modern Photogrammetry*. Wiley, 2001.
- Millefiori, Leonardo M., et al. "COVID-19 impact on global maritime mobility." *Scientific reports* 11.1 (2021): 1-16.
- Mora, Omar E., et al. "Accuracy of stockpile estimates using low-cost sUAS photogrammetry." *International journal of remote sensing* 41.12 (2020): 4512-4529.
- Navalgund, Ranganath R., V. Jayaraman, and P. S. Roy. "Remote sensing applications: An overview." *current science* (2007): 1747-1766.

Nocerino, Erica, and Fabio Menna. "Photogrammetry: linking the world across the water surface." *Journal of Marine Science and Engineering* 8.2 (2020): 128.

Palomer, Albert, Pere Ridaó, and David Ribas. "Inspection of an underwater structure using point-cloud SLAM with an AUV and a laser scanner." *Journal of field robotics* 36.8 (2019): 1333-1344.

"Review of Maritime Transport 2022." *UNCTAD*, 29 Nov. 2022,
<https://unctad.org/webflyer/review-maritime-transport-2022>.

BIOGRAPHY

Paul Stoiber graduated from La Quinta High School, La Quinta, California, in 2015. He received his Bachelor of Science from California State Polytechnic University, Pomona in 2019. He was employed as a Photogrammetrist and Facilities Engineer in the Department of Defense for three years.